ENVIRONMENTAL HEALTH PERSPECTIVES
http://www.ehponline.org

Towards More Comprehensive Projections of Urban Heat-Related Mortality: Estimates for New York City under Multiple Population, Adaptation, and Climate Scenarios

Elisaveta P. Petkova, Jan K. Vink, Radley M. Horton, Antonio Gasparrini, Daniel A. Bader, Joe D. Francis, and Patrick L. Kinney

http://dx.doi.org/10.1289/EHP166

Received: 12 October 2015
Revised: 16 January 2016
Accepted: 13 May 2016
Published: 23 June 2016

Environ Health Perspect DOI: 10.1289/EHP166
Advance Publication: Not Copyedited

Towards More Comprehensive Projections of Urban Heat-Related Mortality: Estimates for New York City under Multiple Population, Adaptation, and Climate Scenarios

Elisaveta P. Petkova[1], Jan K. Vink[2], Radley M. Horton[3], Antonio Gasparrini[4,5], Daniel A. Bader[3], Joe D. Francis[2], and Patrick L. Kinney[6]

[1]National Center for Disaster Preparedness, Earth Institute, Columbia University, New York, New York, USA; [2]Cornell Program on Applied Demographics, Cornell University, Ithaca, New York, USA; [3]Columbia University Center for Climate Systems Research, New York, New York, USA; [4]Department of Social and Environmental Health Research, London School of Hygiene & Tropical Medicine, London, UK; [5]Department of Medical Statistics, London School of Hygiene & Tropical Medicine, London, UK; [6]Department of Environmental Health Sciences, Mailman School of Public Health, Columbia University, New York, New York, USA

Address correspondence to Elisaveta P. Petkova, National Center for Disaster Preparedness, Earth Institute, Columbia University, 215 W. 125th Street, New York, NY 10027 USA. Telephone: (646) 845-2325. E-Mail: epp2109@columbia.edu

Short running title: Projections of urban heat-related mortality

Acknowledgments: This work was supported by the Consortium for Climate Risk in the Urban Northeast (CCRUN), the National Center for Disaster Preparedness (NCDP) (Elisaveta P. Petkova), NIEHS Center Grant ES009089 (Elisaveta P. Petkova and Patrick L. Kinney), and a Methodology Research fellowship from Medical Research Council (Grant ID: MR/M022625/1) (Antonio Gasparrini).

Competing financial interests: The authors declare no competing financial interests.

Abstract

Background: High temperatures have substantial impacts on mortality and, with growing concerns about climate change, numerous studies have developed projections of future heat-related deaths around the world. Projections of temperature-related mortality are often limited by insufficient information necessary to formulate hypotheses about population sensitivity to high temperatures and future demographics.

Objectives: This study has derived projections of temperature-related mortality in New York City by taking into account future patterns of adaptation or demographic change, both of which can have profound influences on future health burdens.

Methods: We adopt a novel approach to modeling heat adaptation by incorporating an analysis of the observed population response to heat in New York City over the course of eight decades. This approach projects heat-related mortality until the end of the 21st century based on observed trends in adaptation over a substantial portion of the 20th century. In addition, we incorporate a range of new scenarios for population change until the end of the 21st century. We then estimate future heat-related deaths in New York City by combining the changing temperature-mortality relationship and population scenarios with downscaled temperature projections from the 33 global climate models (GCMs) and two Representative Concentration Pathways (RCPs).

Results: The median number of projected annual heat-related deaths across the 33 GCMs varied greatly by RCP and adaptation and population change scenario, ranging from 167 to 3331 in the 2080s compared to 638 heat-related deaths annually between 2000 and 2006.

Conclusions: These findings provide a more complete picture of the range of potential future heat-related mortality risks across the 21st century in New York, and highlight the importance of both demographic change and adaptation responses in modifying future risks.

Introduction

High temperatures have long been recognized to have substantial impacts on mortality and, with growing concerns about climate change, numerous studies have projected future heat-related mortality due to climate change in recent years (Baccini et al. 2011; Dessai 2003; Gosling et al. 2009; Hayhoe et al. 2004; Hayhoe 2010; Jackson et al. 2010; Knowlton et al. 2007; Ostro et al. 2012; Peng et al. 2011; Sheridan et al. 2012). Some have characterized the relationships between temperature and mortality over the full temperature spectrum at a given location in order to estimate current and future 'net impact' of temperature on mortality (Doyon et al. 2008; Guest et al. 1999; Martin et al. 2012; Martens 1998; Li et al. 2013a). We chose to focus here on heat-related mortality since adaptation responses to cold would likely be quite different, and to date have not been as thoroughly studied as those for heat. Also, previous work in NYC suggested that increases in heat-related mortality are likely to be substantial and may not be offset by decreases in cold-related mortality (Li et al. 2013a).

Projections of temperature-related mortality are, unfortunately, often limited by insufficient understanding of the population adaptation to heat. To date, relatively few heat-health impact studies have considered future adaptation. Some studies have used temperature-mortality curves from 'analogue cities' that currently experience temperatures similar to those projected to occur in the future at a location of interest (Knowlton et al. 2007; Kalkstein and Green 1997) or temperature-mortality curves from hotter 'analogue summers' that have previously occurred in the same location (Hayhoe et al. 2004) . Other studies have developed scenarios for acclimatization to specific increases in temperatures over time (Dessai 2003, Gosling et al. 2009;

Kalkstein and Green 1997). However, to our knowledge, no previous studies have quantified future adaptation trends based on historical patterns of adaptation in the city under study.

An important question to consider is whether the future population response to high temperatures should be projected based on observations from the present and/or the recent past. Cities are complex adaptive systems (Holland 1995; Lansing 2003) capable of self-organizing in order to adapt to environmental conditions. At the same time, there are limits to social adaptation (Dow et al. 2013) that are yet to be well understood and quantified.

In addition to future changes in climate and population adaptation to heat, future demographics are important determinants of health impacts (Huang et al. 2011). Utilizing multiple population change scenarios is also important for quantifying the range and uncertainty of potential temperature-related health impacts.

We start by developing heat adaptation models that project the population response to heat until 2100 based on eight decades of historical daily temperature and mortality data. The approach is particularly suitable for New York City, which is among the largest cities in the world and has retained a relatively consistent urban shape over the entire historical period covered by this study. We then develop demographic scenarios that characterize potential changes in the city population during the study period. Finally, we calculate future heat-related deaths by combining the derived temperature-mortality relationships and population scenarios with the downscaled temperature projections from the 33 Global Climate Models and two Representative Concentration Pathways (RCPs), RCP4.5 and RCP8.5, developed in support of the Intergovernmental Panel on Climate Change (IPCC)'s Fifth Assessment Report (AR5) (IPCC, 2013).

Methods

Daily Mortality data

The process of the historical daily mortality data preparation and validation was discussed in detail previously (Petkova et al. 2014). Death records prior to 1949 are stored at the New York City Department of Records and Information Services (DORIS). Death indexes for all years between 1900 and 1949, including each documented death in the five New York City boroughs (Bronx, Brooklyn, Manhattan, Queens, and Staten Island) from 1900 to 1948, were scanned by the Genealogy Federation of Long Island (GFLI). Annual numbers of deaths calculated from these records were compared with the numbers published in the New York City Department of Health's annual Summary of Vital Statistics reports. Annual calculated numbers of deaths were between 0.02% and 4.94 % (median 0.95%) higher than those reported in the annual Summary of Vital Statistics reports (Petkova et al. 2014).

Death records for the years after 1950 are stored at the New York City Department of Health (NYC DOH MH) and Mental Hygiene and were not directly accessible or available in digital format for this study.

Daily multiple-cause-of-death mortality data for all five New York City boroughs for 1973-2006 were obtained in collaboration with Joel Schwartz and colleagues at Harvard University School of Public Health from the U.S. National Center for Health Statistics (NCHS).

Temperature data

Daily temperature data before 1949 were obtained for New York Central Park from the United States Historical Climatology Network (USHCN). There were five missing records in the data

prior to 1949 that were substituted with the averages of the previous and following day temperatures. Daily temperature data, also from the New York Central Park station from 1973 onwards were obtained from the National Climatic Data Center (NCDC).

Historical Heat-Mortality Relationships

We used the distributed lag non-linear model (DLNM) module in R (Gasparrini 2011) to characterize the temperature-mortality relationships for each time period. Distributed lag non-linear models allow a simultaneous characterization of the non-linear and lagged effects of temperature on mortality (Armstrong 2006, Gasparrini et al. 2010). Decadal models for 1900-1909 (1900s), 1910-1919 (1910s), 1920-1929 (1920s), 1930-1939 (1930s), 1940-1948 (1940s), 1973-1979 (1970s), 1980-1989 (1980s), 1990-1999 (1990s) and 2000-2006 (2000s) were developed using mean daily temperature and 22 ˚C (corresponding to approximately the 80th percentile of annual temperature) as a reference temperature for calculating relative risk. The temperature-mortality analysis was restricted to the summer months (June to September) in order to focus on heat-related mortality. The model is represented by the following equation:

$$\log[E(y_t)] = \alpha + f(x_t;\boldsymbol{\beta}) + s(t;\boldsymbol{\gamma}) + g(j_t;\boldsymbol{\eta}) + \sum_{p=1}^{6} \delta_p\, I_p(d_t) \quad (1)$$

where:

- $E(y_t)$ is the expected number of deaths at day t
- f is the function modelling the association with *x*, a moving average of temperature over a lag of 3 days (lag 0-3), with parameters $\boldsymbol{\beta}$
- s is the function of time *t* modelling the long term trend with parameters $\boldsymbol{\gamma}$
- g is the function of the day of the year *j* modelling the seasonal trend with parameters $\boldsymbol{\eta}$

- I_p are a series of indicators modelling the association with day of the week d with parameters δ_p

While longer lags have been found to be appropriate in modeling heat-mortality impacts in the beginning of the 20th century due to some immediate partial harvesting following exposure to heat, shorter lags have been found to adequately capture heat effects in recent decades (Petkova et al. 2014). Thus, a lag of 3 days was selected in order to focus on the immediate impact of heat on mortality. We defined f as a cross-basis composed of quadratic spline with 4 degrees of freedom with 2 knots at equally-spaced percentiles of temperature distribution for the exposure-response function, and a natural spline with 2 degrees of freedom with 2 knots for the lag-response function. The functions s and g were defined as natural cubic splines, with 7 degrees of freedom per decade and with 4 degrees of freedom for day in year, respectively.

Temperature Projections

The methods used here are also described in Petkova et al., 2013. Downscaled climate projections were developed using monthly Bias Corrected Spatially Disaggregated (BCSD) data at 1/8° resolution (Maurer et al. 2007). The data are derived from the WCRP CMIP5 multi-model data set and include 33 global climate models (GCMs) used in the Intergovernmental Panel on Climate Change (IPCC)'s Fifth Assessment Report (AR5). The global climate models along with their originating institution and atmospheric resolution are presented in Table 1.

Projections are provided for two representative concentration pathways (RCPs; Moss et al. 2010). The pathways are the basis for near- and long-term climate modeling experiments and make various underlying assumptions about radiative forcing through time, which depends upon future global greenhouse gas and aerosol concentrations, and land use changes.

The two RCPs used in this analysis are RCP4.5 and RCP8.5, the most used amongst the climate modeling community. These two scenarios represent relatively low (4.5) and high (8.5) greenhouse gas projections/radiative forcing through the end of the century. Under RCP4.5, stabilization of greenhouse gas concentrations occurs shortly after 2100, as a product of emissions reduction prior to that time. RCP8.5 is a scenario with increasing emissions through the century, associated with an energy intensive future and limited use of green technologies (van Vuuren et al. 2011).

To develop daily temperature projections, the monthly output for the 1/8° grid box corresponding to New York (Central Park) from the climate models was used to develop change factors for each calendar month based on the difference between a 30-year future average for that calendar month and the same model's 30-year baseline average for that same calendar month (Rosenzweig et al. 2011). The monthly change factors were then applied to the respective observed daily weather data to create a future projection.

The combination of 33 models and 2 RCPs yields 66 synthetic future temperature projections for daily mean temperature from 2010 to 2099 that are based on three 30-year time slices, defined as the 2020s (2010 to 2039), 2050s (2040 to 2069) the 2080s (2070 to 2099).

Population Projections

A comprehensive set of population projections for New York State until 2040 along with a detailed methodology has been previously derived by the Cornell Center for Applied Demographics (Vink 2009).

Projections were developed for this study by establishing a range of assumptions regarding the components of the basic demographic equation based on the Cohort-Component (Smith et al. 2001):

$$POP_t^a = \begin{cases} POP_{t-1}^{a-1} - D_{t-1,t}^a + NM_{t-1,t}^a, & \text{for age } a > 0 \text{ and } t > 0 \\ B_{t-1,t} - D_{t-1,t}^a + NM_{t-1,t}^a, & \text{for age } a = 0 \text{ and } t > 0 \end{cases} \quad (2)$$

Where:

- POP_t^a is the city population age *a* in at point *t* in time
- POP_0^a is the population age *a* at the beginning of the projection according to the Decennial Census 2010. See 2010 Census Summary File 1 (U. S. Census Bureau 2010)
- $B_{t-1,t}$ is the number of births between year before point *t* in time and point *t* and is a function of age specific fertility rates and the number of females at each age
- $D_{t-1,t}^a$ is the number of deaths between year before point *t* in time and point *t* that would otherwise have been age *a* at point *t.* It is a function of age specific mortality rates and the number of people at risk
- $NM_{t-1,t}^a$ is the net migration between year before point *t* in time and point *t* of people that are age *a* at point *t*. Net migration is the difference between the number of people moving in (a function of an age profile and the total level of people moving in) and the number of people moving out (a function of age specific rates and the local population of a certain age)

This set of equations is set up separately by sex.

We defined five different scenarios for projecting future NYC populations by altering the parameters of the equations above. The *Baseline* scenario assumed that all parameters of the model remain constant, that is age specific fertility and mortality rates and age characteristics of migration are all kept constant, but the population ages forward. The *Decreased Mortality* scenario assumed a decrease in age specific mortality rates such that the values reach to 2/3 of the 2010 values in 2100. Life expectancy at birth will increase with 6 years over time under this scenario, which is in line with the mortality assumptions in the recent Census Bureau projections (U. S. Census Bureau 2012). The third scenario, *Increased In-Migration,* assumed that the growth of the domestic in-migration (from other parts of the US to NYC) will be half of the growth of the US population and that the growth of the international in-migration (from outside of the US to NYC) will be half of the growth of the projected international in-migration nationwide (from the Census 2010 projections). The fourth scenario, *Increased Out-Migration*, assumed that the rate of out-migration would increase by 25% over the projection period. The assumptions for the increased in-migration and increased out-migration are rather arbitrary, but aim to strike a balance between reasonable and informative. More radical assumptions would lead to New York City populations that would introduce various complications because of overcrowding or high vacancy rates. Finally, we also used a *Constant*, no-population change scenario in which population and age of the population remains constant at the 2010 level.

Projected Heat-Related Mortality

As previously reported (Petkova et al. 2014), RRs estimated for heat-related mortality were relatively constant during the first part of 20th century, suggesting little adaptation to heat during this period, while RRs decreased from the 1970s to the 2000s, consistent with substantial

adaptation to heat. Specifically, the average relative risk of mortality associated with a daily mean temperature of 29ºC vs. 22ºC during June–September ranged from 1.30 (95% CI: 1.25, 1.36) in the 1910s to 1.43 (95% CI: 1.37, 1.49) in the 1900s. In contrast, predicted average relative risks for the same exposure contrast fell from 1.38 (95%CI: 1.31, 1.44) during 1900–1948 to only 1.15 (95%CI: 1.09, 1.20) during 1973-2006 (p-value <0.001), suggesting rapid adaptation since the 1970s (Petkova et al. 2014). We believe that increased access to air conditioning in recent years was the primary cause of the apparent increase in adaptation. A random-effects meta-regression including a linear term for decade predicted a decrease of 4.6% (95%CI: 2.4%-6.7%) per decade (p-value <0.001) (Petkova et al. 2014).

Since we do not have mortality data from the 1950s and 1960s, we cannot verify the precise onset of the adaptation process (as indicated by the downward shift in the trend for RRs). However, if we assume that access to air conditioning was the major driving force behind heat adaptation, it is plausible to define three stages in the population response to heat: prior to the introduction of domestic air conditioning, during air conditioning penetration and after air conditioning penetration levels reach a steady state. Since 84% of surveyed households in New York City in 2003 already had air conditioning in their homes (U.S. Census Bureau 2004), compared with only 39% in 1979 (U.S. Census Bureau 1978), we assume that the prevalence of air conditioning will reach a steady state level sometime in the near future.

Future heat-related mortality relative risks at each degree Celsius (˚C) were derived for temperatures 25°C and above using the temperature-specific relative risk estimates from the historical decades as described earlier. Decade-specific temperature curves were linearly extrapolated for temperatures up to 41˚C, the highest projected temperature, using the last four

temperature data points of each curve. We chose a sigmoid function to model the decadal change in the heat-mortality response since it permits an accurate approximation of the three stages in the adaptation process:

$$RR_{ADAPT} = RR_{MAX} - \frac{RR_{RANGE}}{1+e^{-\propto *(Y-Y_0)}} \quad (3)$$

The initial level of temperature-specific relative risk (RR_{MAX}) at each temperature was determined by selecting the mean relative risk from the first part of the 20th century, corresponding to the pre-adaptation part of the sigmoid curve. The RR_{RANGE} was derived as the difference between the RR_{MAX} and RR_{MIN}, where RR_{MIN} is the minimal relative risk for a given temperature or the value to which the sigmoidal curve converges. We developed two future adaptation scenarios in addition to a no adaptation scenario: a scenario of high adaptation where the projected RR_{MIN} in 2100 is 80% lower than the RR observed at the same temperature during the 2000s, and a scenario of moderate adaptation where the projected RR_{MIN} in 2100 is 20% lower than the corresponding observed RR during the 2000s. Y represents the year for which RR_{ADAPT} is calculated and Y_0 represents the half decay point, or year in which RR_{MAX} drops by half of the RR_{RANGE}. The steepness of the transition between the periods of no adaptation and complete adaptation is determined by the coefficient α. Both α and Y_0 were subjected to nonlinear least squares optimization using the data points for the last four decades. We are not proposing a scenario assuming 100% adaptation because sub-populations of vulnerable individuals without access to air conditioning or other means of heat relief are likely to continue to exist in the future and thus heat-related mortality may not be completely avoidable.

Future heat-related deaths were calculated as described in Petkova et al. 2013. Here, population change and heat adaptation scenarios were also incorporated into the calculations. The temperature-specific relative risks derived from the *No Adaptation*, *High Adaptation* and *Low Adaptation* scenarios were applied to the daily, downscaled temperature projections until 2100.

Results

Our previous study of heat adaptation patterns in New York City that examined daily temperature and mortality data spanning more than a century in New York City, found no evidence of adaptation during the beginning of the 20th century, but evidence of rapid adaptation in subsequent decades (Petkova et al. 2014). Based on these findings we developed a three-stage model of adaptation. We also developed two future adaptation scenarios, of low and high adaptation, respectively, assuming different levels of adaptation throughout the 21st century. Temperature-specific mortality curves for New York City calculated according to the low and high adaptation scenarios are illustrated in Figure 1. Points represent the relative risks calculated by the DLNM model for each temperature for the decades 1970s-2000s.

In order to characterize possible population change pathways in New York City throughout the 21st century, we developed four new population scenarios, making a range of assumptions about future mortality, in-migration, and out-migration. Population projections (Figure 2) based on the four scenarios developed for this study were used in addition to a no-population change (*Constant*) scenario in deriving assessments of future heat-related mortality. Annual population projections according to each scenario along with the corresponding mortality rates are provided in the Supplemental Material, Table S1.

Finally, we obtained statistically downscaled future mean temperature projections for New York City for 33 global-scale general circulation models (GCMs) used in the Intergovernmental Panel on Climate Change (IPCC)'s Fifth Assessment Report (AR5), and two representative concentration pathways (RCPs), RCP 4.5 and 8.5, representing relatively low and high greenhouse gas projections, respectively. This yielded an ensemble of 66 model/scenario combinations for future health impact calculations.

Future mortality estimates varied greatly depending on the choice of demographic and adaptation scenario. To emphasize the influence of both population change and heat adaptation, we used the 33 climate model median and the two RCPs. Median numbers of projected heat-related deaths across the 33 GCMs used during the 2020s, 2050s and 2080s are summarized by RCP, adaptation scenario and population scenario in Figure 3 and Table 2.

The estimated median number of heat-related deaths across the 33 GCMs is substantially higher under RCP8.5 as the century progresses, and in many cases the number of deaths projected under RCP8.5 is more than twice the corresponding estimate for RCP4.5 under the same time, population, and adaptation scenarios. These findings suggest that the number of deaths would be substantially reduced under the lower emission pathway, RCP4.5. For example, we estimate that by the 2080s, 1494 annual heat-related deaths could be avoided under the *Increased In-Migration/Low Adaptation* scenario, based on 2,771 versus 1,277 projected deaths under RCP8.5 and RCP4.5, respectively (Table 2).

Projected heat-related mortality was highest for the *Increased In-Migration* population scenario followed by the *Baseline*, *Increased Out-Migration*, *Decreased Mortality* and *Constant* population scenarios. As an example, for the 2080s under the RCP8.5/*High Adaptation* scenario,

we projected 804 deaths under the *Increased In-Migration* scenario, 698 deaths under the *Baseline scenario*, 624 deaths under both the *Increased Out-Migration* and *Decreased Mortality* scenarios and 379 deaths under the *Constant* population scenario.

Increasing levels of adaptation reduced the number of projected deaths substantially. For instance, by the 2080s, 3331, 2271 and 804 deaths could occur under RCP8.5 and the *Increased In-Migration/No Adaptation*, *Increased In-Migration/Low Adaptation* and *Increased In-Migration/High Adaptation,* respectively. As another example, during the 2020s and under the RCP 4.5, the median number of heat-related deaths across the 33 GCMs was 370 for the *Constant* population scenario and *No Adaptation* and 149 for the same scenario and *High Adaptation.*

Discussion

To our knowledge, this study is the first to present projections of heat-related mortality until the end of the 21st century while incorporating assumptions of heat adaptation based on historical mortality data spanning over a century. Our adaptation model characterized long term trends in the population response to heat and under alternative assumptions about the limits to future adaptation. There is considerable agreement that limits to adaptation to climate change exist and are often defined by interactions between climate change and biophysical and socioeconomic constraints among other factors (Klein et al. 2014). Quantifying the potential limits and obstacles to climate change adaptation as they relate to various health outcomes is critical for achieving optimal resource allocation and long term planning.

Projecting future population adaptation to heat is among the most important challenges in assessing the burden of heat-related mortality under a changing climate. Here, we have proposed a novel approach to modeling heat adaptation that allows the consideration of observed trends in adaptation since the beginning of the 20th century. Since our previous findings suggested that there was no adaptation to heat in New York City during the first part of the 20th century (Petkova et al. 2014), we used the mean relative risk estimated for the early part of the 20th century to anchor the upper segment of the sigmoidal adaptation function (equation 3) for that period. We used the declining relative risks estimated for recent decades to characterize adaptation that occurred as the prevalence of air conditioning increased, and extrapolated this decline to 2100 under two different adaptation scenarios representing modest and more substantial increases in adaptation from the 2010 level.

Although population change is considered to be among the most important factors in estimating future temperature impacts, future demographics are often not taken into account because location-specific population projections are generally not readily available beyond several decades. To address this issue, we developed new population change scenarios to apply to our projections of heat-related mortality. Finally, we combined the developed population and heat adaptation scenarios with temperature projections from multiple GCMs and two RCPs in order to derive a comprehensive assessment for heat-related mortality until the end of the 21st century.

Annual future mortality estimates varied greatly by RCP, as well as by population change and adaptation scenario. For instance, the *Constant/High Adaptation* scenario produced the lowest death estimates, projecting 167 and 379 heat-related deaths during the 2080s under the RCP4.5 and the RCP 8.5, respectively. The *Increased In-Migration/No Adaptation* scenario produced the

highest mortality estimates under the RCP 8.5, projecting 555 and 3331 deaths during the 2020s and 2080s, respectively.

Both the heat adaptation and demographic scenarios have several limitations. First, our model of heat-related mortality over time was based on an empirical fit to historical data and extrapolation using a sigmoidal curve into the future. We did not identify and incorporate causal factors like air conditioning use into the projection of future heat response. Future research that focuses on characterizing the impact of heat over time among vulnerable populations would be particularly useful in improving the utility of the adaptation models. In addition, studies quantifying the impact of various public health interventions such as heat warning systems, cooling centers and other preventive measures on heat-related mortality would be valuable for the further development of this work. Another important limitation of the study is that decade-specific mortality vs. temperature curves were linearly extrapolated to high temperatures projected to occur under changing climate (e.g. 41°C) for which no historical mortality data exist. This may underestimate mortality impacts at such very high temperatures, particularly during the initial exposures of the populations to temperatures that they have not previously experienced. Studies of mortality responses in non-acclimatized populations would be particularly useful in better characterizing heat impacts at very high temperatures. Finally, we acknowledge that the assumptions underlying the two adaptation scenarios developed for this study were arbitrary, but we believe they capture a reasonable range of potential future adaptation, from modest (20%) to substantial (80%). More data over a longer time period will be needed to determine which end of this range is most realistic.

Although we believe that the assumptions of the demographic models developed for this work are reasonable, they are based on historical trends that may or may not continue. Population projections are rarely developed beyond several decades, especially on a finer, city-level geographical scale. Given the increasing importance of projecting population health impacts under a changing climate, additional work focused on developing and validating long-term population projections will be of critical importance for improving the accuracy of projecting heat-related mortality and other health impacts. Nevertheless, by including five different population scenarios, our study is among the first to examine sensitivity to this important assumption.

The methods and findings of this study may be particularly relevant to estimating heat-related mortality in cities currently experiencing heat impacts and increasing urbanization and/or population growth. Since the choice of adaptation scenario affected the number of projected heat-related deaths substantially, improved understanding of heat adaptation is necessary in order to refine projections. Nonetheless, the substantial reduction of heat-related mortality, particularly under the *High Adaptation* scenario provides evidence of the importance of public policy measures leading to continuous heat adaptation. Finally, the number of median annual heat-related deaths calculated across all models under RCP8.5 was in many instances over twice as high as the number of deaths projected under RCP 4.5. This difference underlines the magnitude of the potential public health benefit associated with reducing greenhouse gas concentrations in the atmosphere.

References

Armstrong B. 2006. Models for the relationship between ambient temperature and daily mortality. Epi 17:624-631.

Baccini M, Kosatsky T, Analitis A, Anderson HR, D'Ovidio M, Menne B, Michelozzi P, Biggeri A, PHEWE Collaborative Group. 2011. Impact of heat on mortality in 15 European cities: attributable deaths under different weather scenarios. J Epi Comm Hlth 65:64-70.

Bi D, Dix M, Marsland SJ, O'Farrell S, Rashid H, Uotila P, Hirst A, Kowalczyk E, Golebiewski M, Sullivan A, Yan H. 2013b. The ACCESS coupled model: description, control climate and evaluation. Aust Meteorol Oceanogr J 63: 41-64.

Collins WD, Rasch PJ, Boville BA, Hack JJ, McCaa JR, Williamson DL, Briegleb BP, Bitz CM, Lin SJ, Zhang M. 2006. The formulation and atmospheric simulation of the Community Atmosphere Model version 3 (CAM3). J Clim 19:2144-2161.

Collins WJ, Bellouin N, Doutriaux-Boucher M, Gedney N, Halloran P, Hinton T, Hughes J, Jones CD, Joshi M, Liddicoat S, Martin G. 2011. Development and evaluation of an Earth-system model–HadGEM2. Geosci Model Dev 4:1051-1075.

Davies T, Cullen MJ, Malcolm AJ, Mawson MH, Staniforth A, White AA, Wood N. 2005. A new dynamical core for the Met Office's global and regional modelling of the atmosphere. Q J R Meteorol Soc 131:1759-1782.

Delworth TL, Broccoli AJ, Rosati A, Stouffer RJ, Balaji V, Beesley JA, Cooke WF, Dixon KW, Dunne J, Dunne KA, Durachta JW. 2006. GFDL's CM2 global coupled climate models. Part I: Formulation and simulation characteristics. J Clim 19:643-674.

Dessai S. 2003. Heat stress and mortality in Lisbon Part II. An assessment of the potential impacts of climate change. Intl J Biometeorol 48:37-44.

Donner LJ, Wyman BL, Hemler RS, Horowitz LW, Ming Y, Zhao M, Golaz JC, Ginoux P, Lin SJ, Schwarzkopf MD, Austin J. 2011. The dynamical core, physical parameterizations, and basic simulation characteristics of the atmospheric component AM3 of the GFDL global coupled model CM3. J Clim 24:3484-3519.

Dow K, Berkhout F, Preston BL, Klein RJ, Midgley G, Shaw MR. 2013. Limits to adaptation. Nature Clim Change 3:305-307.

Doyon B, Bélanger D, Gosselin P. 2008. The potential impact of climate change on annual and seasonal mortality for three cities in Quebec, Canada. Intl J Hlth Geographics 7:1-12.

Dufresne JL, Foujols MA, Denvil S, Caubel A, Marti O, Aumont O, Balkanski Y, Bekki S, Bellenger H, Benshila R, Bony S. 2013. Climate change projections using the IPSL-CM5 Earth System Model: from CMIP3 to CMIP5. Clim Dyn 40:2123-2165; doi:10.1007/s00382-012- 1636-1

Dunne JP, John JG, Shevliakova E, Stouffer RJ, Krasting JP, Malyshev SL, Milly PC, Sentman LT, Adcroft AJ, Cooke W, Dunne KA. 2013. GFDL's ESM2 global coupled climate–Carbon Earth System Models. Part II: Carbon system formulation and baseline simulation characteristics. J Clim 2013 26:2247-2267.

Gasparrini A, Armstrong B, Kenward MG. 2010. Distributed lag non-linear models. Stat in Med 29:2224-2234.

Gasparrini A. 2011. Distributed lag linear and non-linear models in R: the package DLNM. J Stat Software 43:1-20.

Genealogy Federation of Long Island (GFLI). Available: http://freepages.genealogy.rootsweb.ancestry.com/~gfli/ [accessed 10 May 2016].

Gent PR, Danabasoglu G, Donner LJ, Holland MM, Hunke EC, Jayne SR, Lawrence DM, Neale RB, Rasch PJ, Vertenstein M, Worley PH. 2011. The community climate system model version 4. J Clim 24:4973-4991.

Gosling SN, McGregor GR, Lowe JA. 2009. Climate change and heat-related mortality in six cities Part 2: climate model evaluation and projected impacts from changes in the mean and variability of temperature with climate change. Intl J of Biometeor 53:31-51.

Guest CS, Wilson K, Woodward AJ, Hennessy K, Kalkstein LS, Skinner C, McMichael AJ. 1999. Climate and mortality in Australia: retrospective study, 1979-1990, and predicted impacts in five major cities in 2030. Clim Res 13:1-15.

Hayhoe K, Sheridan S, Kalkstein L, Greene S. 2010. Climate change, heat waves, and mortality projections for Chicago. J Great Lakes Res 36:65-73.

Hayhoe K, Cayan D, Field CB, Frumhoff PC, Maurer EP, Miller NL, Moser SC, Schneider SH, Cahill KN, Cleland EE, Dale L. 2004. Emissions pathways, climate change, and impacts on California. In: Proceedings of the National Academy of Sciences of the United States of America. Vol 101:12422-7.

Holland, JH. 1995. Hidden Order: How Adaptation Builds Complexity. Perseus Books.

Hourdin F, Foujols MA, Codron F, Guemas V, Dufresne JL, Bony S, Denvil S, Guez L, Lott F, Ghattas J, Braconnot P. 2013a. Impact of the LMDZ atmospheric grid configuration on the climate and sensitivity of the IPSL-CM5A coupled model. Clim Dyn 40:2167-2192.

Hourdin F, Grandpeix JY, Rio C, Bony S, Jam A, Cheruy F, Rochetin N, Fairhead L, Idelkadi A, Musat I, Dufresne JL. 2013b. LMDZ5B: the atmospheric component of the IPSL climate model with revisited parameterizations for clouds and convection. Clim Dyn 40:2193-2222.

Huang C, Barnett AG, Wang X, Vaneckova P, FitzGerald G, Tong S. 2011. Projecting future heat-related mortality under climate change scenarios: a systematic review. Env Hlth Pers 119:1681.

Hurrell JW, Holland MM, Gent PR, Ghan S, Kay JE, Kushner PJ, Lamarque JF, Large WG, Lawrence D, Lindsay K, Lipscomb WH. 2013. The community earth system model: a framework for collaborative research. Bull Am Meteorol Soc 94:1339-1360; doi:10.1175/BAMS-D-12– 00121.

Iversen T, Bentsen M, Bethke I, Debernard JB, Kirkevåg A, Seland Ø, Drange H, Kristjansson JE, Medhaug I, Sand M, Seierstad IA. 2013. The Norwegian earth system model, NorESM1-M—Part 2: climate response and scenario projections. Geosci Model Dev 6:389-415.

Jackson JE, Yost MG, Karr C, Fitzpatrick C, Lamb BK, Chung SH, Chen J, Avise J, Rosenblatt RA, Fenske RA. 2010. Public health impacts of climate change in Washington State: projected mortality risks due to heat events and air pollution. Clim Change 102:159-86.

Kalkstein LS, Greene JS. 1997. An evaluation of climate/mortality relationships in large US cities and the possible impacts of a climate change. Env Hlth Pers 105:84.

Kirkevåg A, Iversen T, Seland Ø, Hoose C, Kristjánsson JE, Struthers H, Ekman AM, Ghan S, Griesfeller J, Nilsson ED, Schulz M. 2013. Aerosol–climate interactions in the Norwegian Earth System Model–NorESM1-M. Geosci Model Dev 6:207-244.

Klein, R.J.T., G.F. Midgley, B.L. Preston, M. Alam, F.G.H. Berkhout, K. Dow, and M.R. Shaw, 2014: Adaptation opportunities, constraints, and limits. In: Climate Change 2014: Impacts, Adaptation, and Vulnerability. Part A: Global and Sectoral Aspects. Contribution of Working Group II to the Fifth Assessment Report of the Intergovernmental Panel on Climate Change [Field, C.B., V.R. Barros, D.J. Dokken, K.J. Mach, M.D. Mastrandrea, T.E. Bilir, M. Chatterjee, K.L. Ebi, Y.O. Estrada, R.C. Genova, B. Girma, E.S. Kissel, A.N. Levy, S. MacCracken, P.R. Mastrandrea, and L.L. White (eds.)]. Cambridge University Press, Cambridge, United Kingdom and New York, NY, USA, p. 899-943.

Knowlton K, Lynn B, Goldberg RA, Rosenzweig C, Hogrefe C, Rosenthal JK, Kinney PL. 2007. Projecting heat-related mortality impacts under a changing climate in the New York City region. Am J Pub Hlth 97:2028-2034.

Lansing JS. 2003. Complex adaptive systems. Ann Rev Anthro 183-204.

Li L, Lin P, Yu Y, Wang B, Zhou T, Liu L, Liu J, Bao Q, Xu S, Huang W, Xia K. 2013c. The flexible global ocean-atmosphere-land system model, Grid-point Version 2: FGOALS-g2. Adv Atmos Sci 30:543-560.

Li T, Horton RM, Kinney PL. 2013a. Projections of seasonal patterns in temperature-related deaths for Manhattan, New York. Nature Clim Change 3:717-721.

Li L, Wang B, Dong L, Liu L, Shen S, Hu N, Sun W, Wang Y, Huang W, Shi X, Pu Y. 2013b. Evaluation of grid-point atmospheric model of IAP LASG version 2 (GAMIL2). Adv Atmos Sci 30:855-867.

Long MC, Lindsay K, Peacock S, Moore JK, Doney SC. 2013. Twentieth-century oceanic carbon uptake and storage in CESM1 (BGC). J Clim 26:6775-6800.

Martens WJ. 1998. Climate change, thermal stress and mortality changes. Soc Sci Med 46:331-344.

Martin SL, Cakmak S, Hebbern CA, Avramescu ML, Tremblay N. 2012. Climate change and future temperature-related mortality in 15 Canadian cities. Intl J of Biometeorol 56:605-619.

Maurer EP, Brekke L, Pruitt T, Duffy PB. 2007. Fine-resolution climate projections enhance regional climate change impact studies. Eos Trans Am Geophys Union 88:504. doi:10.1029/2007EO47000

Moss RH, Edmonds JA, Hibbard KA, Manning MR, Rose SK, Van Vuuren DP, Carter TR, Emori S, Kainuma M, Kram T, Meehl GA. 2010. The next generation of scenarios for climate change research and assessment. Nature 463:747-756.

Myhre G, Shindell D, Bréon FM, Collins W, Fuglestvedt J, Huang J, Koch D, Lamarque JF, Lee D, Mendoza B, Nakajima T. 2013. Climate Change 2013: the physical science basis. Contribution of Working Group I to the Fifth Assessment Report of the Intergovernmental Panel on Climate Change. K., Tignor, M., Allen, SK, Boschung, J., Nauels, A., Xia, Y., Bex, V., and Midgley, PM, Cambridge University Press Cambridge, United Kingdom and New York, NY, USA. 1535 pp, doi:10.1017/CBO9781107415324.

National Center for Health Statistics (NCHS). 2016. Mortality Data. Available: www.cdc.gov/nchs/nvss/deaths.htm [accessed 10 May 2016].

National Climatic Data Center (NCDC). Climate Data Online. Available: https://www.ncdc.noaa.gov/cdo-web/ [accessed 10 May 2016].

Neale RB, Richter J, Park S, Lauritzen PH, Vavrus SJ, Rasch PJ, Zhang M. 2013. The mean climate of the Community Atmosphere Model (CAM4) in forced SST and fully coupled experiments. J Clim 26:5150-5168.

New York City Department of Health and Mental Hygiene (NYC DOH MH) Death Certificates. Available: http://www1.nyc.gov/site/doh/services/death-certificates.page [accessed 10 May 2016].

New York City Department of Records and Information Services (DORIS). The Vital Records Collection at the Municipal Archives. Available: http://www.nyc.gov/html/records/html/archives/genealogy.shtml [accessed 10 May 2016].

Ostro B, Barrera-Gómez J, Ballester J, Basagaña X, Sunyer J. 2012. The impact of future summer temperature on public health in Barcelona and Catalonia, Spain. Intl J of Biometeorol 56:1135-1144.

Peng RD, Bobb JF, Tebaldi C, McDaniel L, Bell ML, Dominici F. 2011. Toward a quantitative estimate of future heat wave mortality under global climate change. Env Hlth Pers 119:701-706.

Petkova EP, Horton RM, Bader DA, Kinney PL. 2013. Projected heat-related mortality in the US urban northeast. Intl J Env Res Pub Hlth 10:6734-6747.

Petkova EP, Gasparrini A, Kinney PL. 2014. Heat and mortality in New York City since the beginning of the 20th century. Epidemiology 25:554-560.

Rosenzweig C, Solecki W, DeGaetano, A. 2011. The ClimAID integrated assessment for effective climate change adaptation in New York State. Ann N Y Acad Sci 1244: 2–649.

Rotstayn LD, Lohmann U. 2002. Simulation of the tropospheric sulfur cycle in a global model with a physically based cloud scheme. J Geophys Res: Atmos 107

Schmidt GA, Ruedy R, Hansen JE, Aleinov I, Bell N, Bauer M, Bauer S, Cairns B, Canuto V, Cheng Y, Del Genio A. 2006. Present-day atmospheric simulations using GISS ModelE: Comparison to in situ, satellite, and reanalysis data. J Clim 19:153-192.

Scoccimarro E, Gualdi S, Bellucci A, Sanna A, Giuseppe Fogli P, Manzini E, Vichi M, Oddo P, Navarra A. 2011. Effects of tropical cyclones on ocean heat transport in a high-resolution coupled general circulation model. J Clim 24:4368-4384.

Sheridan SC, Allen MJ, Lee CC, Kalkstein LS. 2012. Future heat vulnerability in California, Part II: projecting future heat-related mortality. Clim Change 115:311-326.

Smith SK, Tayman J, Swanson D.A. 2001. State and local population projections: methodology and analysis. New York: Kluwer Academic/Plenum Publishers.

Stevens B, Giorgetta M, Esch M, Mauritsen T, Crueger T, Rast S, Salzmann M, Schmidt H, Bader J, Block K, Brokopf R. 2013. Atmospheric component of the MPI-M Earth System Model: ECHAM6. J Adv Model Earth Syst 5:146-172. doi:10.1002/jame.20015.

Tjiputra JF, Roelandt C, Bentsen M, Lawrence DM, Lorentzen T, Schwinger J, Seland Ø, Heinze C. 2013. Evaluation of the carbon cycle components in the Norwegian Earth System Model (NorESM). Geosci Model Dev 6:301-325.

U.S. Census Bureau. 1978. Housing characteristics for selected metropolitan areas. Annual housing survey: 1976 Washington, D.C.

U.S. Census Bureau. 2004. American Housing Survey for the New York-Nassau-Suffolk-Orange Metropolitan Area: 2003. Available: https://www.census.gov/prod/2004pubs/h170-03-53.pdf [accessed 12 May 2016].

U. S. Census Bureau. 2010. Total New York City Population. 2010 Census Summary File 1. Available: http://factfinder.census.gov/bkmk/table/1.0/en/DEC/10_SF1/PCT12/1600000US3651000 [accessed 12 May 2016].

U. S. Census Bureau. 2012. 2012 National Population Projections: Methodology and Assumptions. Available: http://www.census.gov/population/projections/files/methodology/methodstatement12.pdf [accessed 10 May 2016].

U.S. Historical Climatology Network (USHCN). Available: https://www.ncdc.noaa.gov/data-access/land-based-station-data/land-based-datasets/us-historical-climatology-network-ushcn [accessed 10 May 2016].

van Vuuren DP, Edmonds J, Kainuma M, Riahi K, Thomson A, Hibbard K, Hurtt GC, Kram T, Krey V, Lamarque JF, Masui T. 2011. The representative concentration pathways: an overview. Clim Change 109:5-31.

Vink J. 2009. New York population projection by age and sex: county projections 2005-2035 Model description. Program on Applied Demographics: Cornell University.

Voldoire A, Sanchez-Gomez E, y Mélia DS, Decharme B, Cassou C, Sénési S, Valcke S, Beau I, Alias A, Chevallier M, Déqué M. 2013. The CNRM-CM5. 1 global climate model: description and basic evaluation. Clim Dyn 40:2091-2121.

Volodin EM, Dianskii NA, Gusev AV. 2010. Simulating present-day climate with the INMCM4. 0 coupled model of the atmospheric and oceanic general circulations. Izvestiya, Atmos Ocean Phys 46:414-431.

von Salzen K, Scinocca JF, McFarlane NA, Li J, Cole JN, Plummer D, Verseghy D, Reader MC, Ma X, Lazare M, Solheim L. 2013. The Canadian fourth generation atmospheric global climate model (CanAM4). Part I: representation of physical processes. Atmos Ocean 51:104-125.

Watanabe M. 2008. Two regimes of the equatorial warm pool. Part I: A simple tropical climate model. J Clim 21:3533-3544.

Watanabe M, Chikira M, Imada Y, Kimoto M. 2011. Convective control of ENSO simulated in MIROC. J Clim 24:543-562.

Watanabe M, Suzuki T, O'ishi R, Komuro Y, Watanabe S, Emori S, Takemura T, Chikira M, Ogura T, Sekiguchi M, Takata K. 2010. Improved climate simulation by MIROC5: mean states, variability, and climate sensitivity. J Clim 23:6312-6335.

Wu T. 2012. A mass-flux cumulus parameterization scheme for large-scale models: Description and test with observations. Clim Dyn 38:725-744.

Yukimoto S, Adachi Y, Hosaka M, Sakami T, Yoshimura H, Hirabara M, Tanaka TY, Shindo E, Tsujino H, Deushi M, Mizuta R. 2012. A new global climate model of the Meteorological Research Institute: MRI-CGCM3—model description and basic performance. J Meteorol Soc Jpn 90A:23-64.

Table 1. IPCC AR5 GCMs used in this study. The models were developed by 22 modeling centers (left column). Some centers support multiple GCMs, and/or versions of their GCM.

Modeling Center	Institute ID	Model Name	Atmospheric Resolution (lat × lon)	References
Commonwealth Scientific and Industrial Research Organization (CSIRO) and Bureau of Meteorology (BOM), Australia	CSIRO-BOM	ACCESS1.0 ACCESS1.3	1.25 × 1.875 1.25 × 1.875	Bi et al. 2013
Beijing Climate Center, China Meteorological Administration	BCC	BCC-CSM1.1 BCC-CSM1.1(m)	2.8 × 2.8 1.1 × 1.1	Wu 2012
College of Global Change and Earth System Science, Beijing Normal University	GCESS	BNU-ESM	2.8 × 2.8	
Canadian Centre for Climate Modelling and Analysis	CCCMA	CanESM2	2.8 × 2.8	Von Salzen et al. 2013
National Center for Atmospheric Research	NCAR	CCSM4	0.9 × 1.25	Gent et al. 2011; Neale et al. 2013
Community Earth System Model Contributors	NSF-DOE-NCAR	CESM1(BGC) CESM1(CAM5)	0.9 × 1.25 0.9 × 1.25	Long et al. 2013; Neale et al. 2013; Hurrell et al. 2013
Centro Euro-Mediterraneo per l Cambiamenti Climatici	CMCC	CMCC-CM	0.75 × 0.75	Scoccimarro et al. 2011; Roeckner et al. 2006
Centre National de Recherches Météorologiques/Centre Européen de Recherche et Formation Avancée en Calcul Scientifique	CNRM-CEFRACS	CNRM-CM5	1.4 × 1.4	Voldoire et al. 2013
Commonwealth Scientific and Industrial Research Organization in collaboration with Queensland Climate Change Centre of Excellence	CSIRO-QCCE	CSIRO-Mk3.6.0	1.9 × 1.9	Rotstayn et al. 2012
LASG, Institute of Atmospheric Physic, Chinese Academy of Sciences and CESS, Tsinghua University	LASG-CESS	FGOALS-g2	2.8 × 2.8	Li et al. 2013b; Li et al. 2013c
The First Institute of Oceanography, SOA, China	FIO	FIO-ESM	2.8 × 2.8	Collins et al. 2006
NOAA Geophysical Fluid Dynamics Laboratory	NOAA GFDL	GFDL-CM3 GFDL-ESM2G GFDL-ESM2M	2.0 × 2.5 2.0 × 2.5 2.0 × 2.5	Donner et al. 2011; Dunne et al. 2013; Delworth et al. 2006
NASA Goddard Institute for Space Studies	NASA GISS	GISS-E2-R	2.0 × 2.5	Schmidt et al. 2006
National Institute of Meteorological Research/Korea Meteorological Administration	NIMR/KMA	HadGEM2-AO	1.25 × 1.875	Collins et al. 2011; Davies et al. 2005
Met Office Hadley Centre (additional HadGEM2-ES realizations contributed by Instituto Nacional de	MOHC (additional	HadGEM2-CC HadGEM2-ES	1.25 × 1.875 1.25 × 1.875	Collins et al., 2011; Davies et al. 2005

Pesquisas Espaciais)	realizations by INPE)			
Institute for Numerical Mathematics	INM	INM-CM4	1.5 × 2.0	Volodin et al. 2010
Institut Pierre-Simon Laplace	IPSL	IPSL-CM5A-LR IPSL-CM5A-MR IPSL-CM5B-LR	1.9 × 3.75 1.3 × 2.5 1.9 × 3.75	Dufresne et al., 2012; Hourdin et al. 2013a; Hourdin et al. 2013b
Japan Agency for Marine-Earth Science and Technology, Atmosphere and Ocean Research Institute (The University of Tokyo), and National Institute for Environmental Studies)	MIROC	MIROC-ESM MIROC-ESM-CHEM	2.8 × 2.8 2.8 × 2.8	Watanabe et al. 2011; Watanabe 2008
Atmosphere and Ocean Research Institute (The University of Tokyo), National Institute for Environmental Studies, and Japan Agency for Marine-Earth Science and Technology	MIROC	MIROC5	1.4 × 1.4	Watanabe et al. 2010
Max Planck Institute for Meteorology	MPI-M	MPI-ESM-MR MPI-ESM-LR	1.9 × 1.9 1.9 × 1.9	Stevens et al. 2013
Meteorological Research Institute	MRI	MRI-CGCM3	1.1 × 1.1	Yukimoto et al. 2012
Norwegian Climate Centre	NCC	NorESM1-M NorESM1-ME	1.9 × 2.5 1.9 × 2.5	Iversen et al. 2013; Kirkevåg et al. 2013; Tjiputra et al. 2013

Table 2. Median number of projected heat-related deaths in New York City across the 33 GCMs used in this study for the 2020s (2010 to 2039), 2050s (2040 to 2069) and 2080s (2070 to 2099) by RCP, adaptation scenario and population scenario. Heat adaptation scenarios include: *(1)High Adaptation:* Adaptation, as measured by *RRmin* or the minimal relative risk for a given temperature to be reached by the year 2100, projected to reach a value 80% lower compared to RR calculated at each degree Celsius (˚C) during the 2000s*; (2)Low Adaptation:* Adaptation, as measured by *RRmin* or the minimal relative risk for a given temperature to be reached by the year 2100, projected to reach a value 20% lower compared to RR calculated at each degree Celsius (˚C) during the 2000s and *(3)No Adaptation:* Future adaptation does not occur. Adaptation, as measured by *RRmin* or the minimal relative risk for a given temperature to be reached by the year 2100, remains the same as the RR calculated at each degree Celsius (˚C) during the 2000s. Population scenarios include: *(1) Baseline:* assumed that all parameters of the model remain constant, that is age specific fertility and mortality rates and age characteristics of migration are all kept constant, but the population ages forward; (2) *Decreased Mortality*: assumed a decrease in age specific mortality rates such that the values reach to 2/3 of the 2010 values by 2100; (3) *Increased In-Migration*: assumed that the growth of the domestic in-migration (from other parts of the US to NYC) will be half of the growth of the US population and that the growth of the international in-migration (from outside of the US to NYC) will be half of the growth of the projected international in-migration nationwide; (4) *Increased Out-Migration*: assumed that the rate of out-migration would increase by 25% over the projection period; and (5) *Constant*: assumed that population and age of the population remains constant at the 2010 level. For reference, there were 638 deaths annually between 2000 and 2006.

		RCP 4.5			**RCP 8.5**		
Period	**Population Scenario**	*No Adaptation*	*Low Adaptation*	*High Adaptation*	*No Adaptation*	*Low Adaptation*	*High Adaptation*
2020s	*Baseline*	492	412	191	549	460	215
2050s	*Baseline*	1084	891	267	1449	1196	365
2080s	*Baseline*	1348	1109	308	2893	2407	698
2020s	*Decreased Mortality*	472	395	184	527	442	207
2050s	*Decreased Mortality*	1001	823	247	1339	1104	338
2080s	*Decreased Mortality*	1205	991	275	2585	2151	624
2020s	*Increased In-Migration*	497	416	193	555	465	217
2050s	*Increased In-Migration*	1151	946	283	1539	1270	387

2080s	*Increased In-Migration*	1552	1277	354	3331	2771	804
2020s	*Increased Out-Migration*	489	409	190	546	457	214
2050s	*Increased Out-Migration*	1040	855	257	1391	1147	351
2080s	*Increased Out-Migration*	1206	991	275	2587	2152	624
2020s	*Constant*	370	311	149	413	347	167
2050s	*Constant*	608	500	150	813	671	205
2080s	*Constant*	733	603	167	1573	1309	379

Figure Legends

Figure 1. Temperature-specific mortality curves for New York City, 1900-2100 **(a)** Adaptation model assumes that temperature-specific relative risks will decrease by an additional 20% *(Low Adaptation)* between 2010 and 2100 compared to the 2000s **(b)** Adaptation model assumes that temperature-specific relative risks will decrease by an additional 80% (*High Adaptation*) between 2010 and 2100 compared to the 2000s. Points represent the relative risks (RRs) calculated by the distributed lag non-linear model (DLNM) for each temperature for the 1970s (1973–1979), 1980s (1980–1989), 1990s (1990–1999), and 2000s (2000–2006). RRs were calculated for June-September using a model with a quadratic spline with 4 degrees of freedom and 22°C as a reference temperature.
Panel A: Low Adaptation
Panel B: High Adaptation

Figure 2. New York City population by 2100 calculated according the five population scenarios developed for this study: (1) *Baseline*: assumed that all parameters of the model remain constant, that is age specific fertility and mortality rates and age characteristics of migration are all kept constant, but the population ages forward; (2) *Decreased Mortality*: assumed a decrease in age specific mortality rates such that the values reach to 2/3 of the 2010 values by 2100; (3) *Increased In-Migration*: assumed that the growth of the domestic in-migration (from other parts of the US to NYC) will be half of the growth of the US population and that the growth of the international in-migration (from outside of the US to NYC) will be half of the growth of the projected international in-migration nationwide; (4) *Increased Out-Migration*: assumed that the rate of out-migration would increase by 25% over the projection period; and (5) *Constant*: assumed that population and age of the population remains constant at the 2010 level.

Figure 3. Median annual projected heat-related deaths in New York City according the **(a)** RCP 4.5 and **(b)** RCP8.5 during the 2020s (2010 to 2039), 2050s (2040 to 2069) the 2080s (2070 to 2099) across 33 global climate models (GCMs). The corresponding numeric data are provided in Table 2. Heat adaptation scenarios are indicated by circle size and include: *(1)High Adaptation:* Adaptation, as measured by *RRmin* or the minimal relative risk for a given temperature to be reached by the year 2100, projected to reach a value 80% lower compared to RR calculated at

each degree Celsius (˚C) during the 2000s*; (2)Low Adaptation:* Adaptation, as measured by *RRmin* or the minimal relative risk for a given temperature to be reached by the year 2100, projected to reach a value 20% lower compared to RR calculated at each degree Celsius (˚C) during the 2000s and *(3)No Adaptation:* Future adaptation does not occur. Adaptation, as measured by *RRmin* or the minimal relative risk for a given temperature to be reached by the year 2100, remains the same as the RR calculated at each degree Celsius (˚C) during the 2000s. Population scenarios are indicated by color and include: *(1) Baseline:* assumed that all parameters of the model remain constant, that is age specific fertility and mortality rates and age characteristics of migration are all kept constant, but the population ages forward; (2) *Decreased Mortality*: assumed a decrease in age specific mortality rates such that the values reach to 2/3 of the 2010 values by 2100; (3) *Increased In-Migration*: assumed that the growth of the domestic in-migration (from other parts of the US to NYC) will be half of the growth of the US population and that the growth of the international in-migration (from outside of the US to NYC) will be half of the growth of the projected international in-migration nationwide; (4) *Increased Out-Migration*: assumed that the rate of out-migration would increase by 25% over the projection period; and (5) *Constant*: assumed that population and age of the population remains constant at the 2010 level. For reference, there were 638 deaths annually between 2000 and 2006.

Panel A: RCP 4.5

Panel B: RCP 8.5

Figure 1.

Panel A

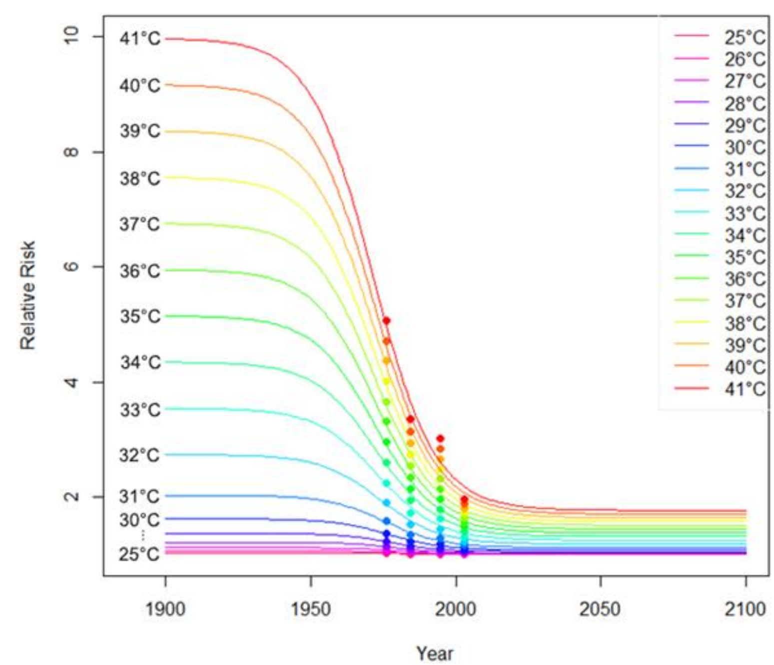

Panel B

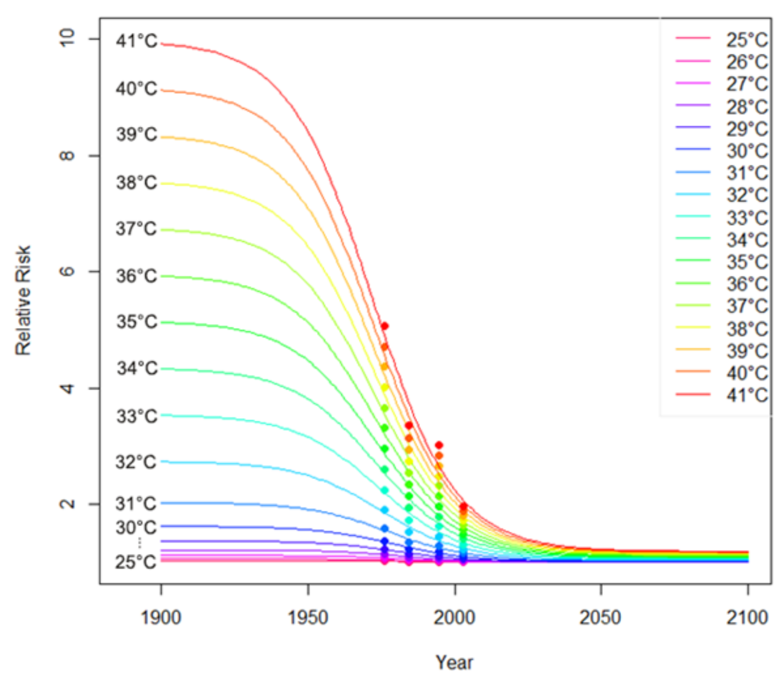

Environ Health Perspect DOI: 10.1289/EHP166
Advance Publication: Not Copyedited

Figure 2.

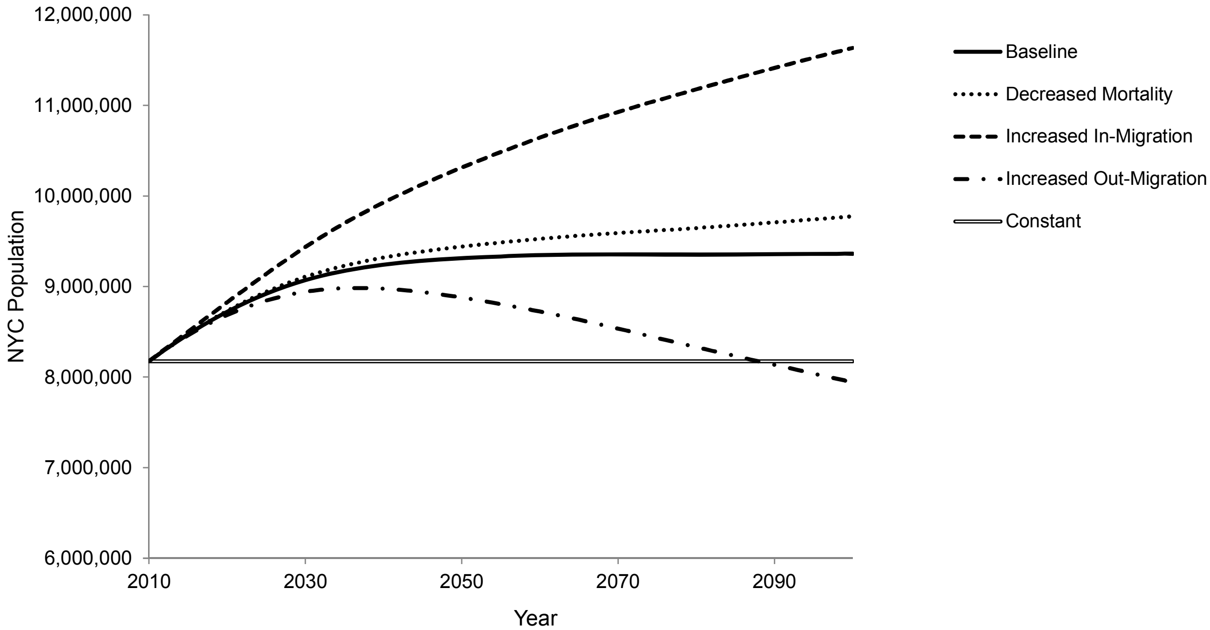

Environ Health Perspect DOI: 10.1289/EHP166
Advance Publication: Not Copyedited

Figure 3.

Panel A

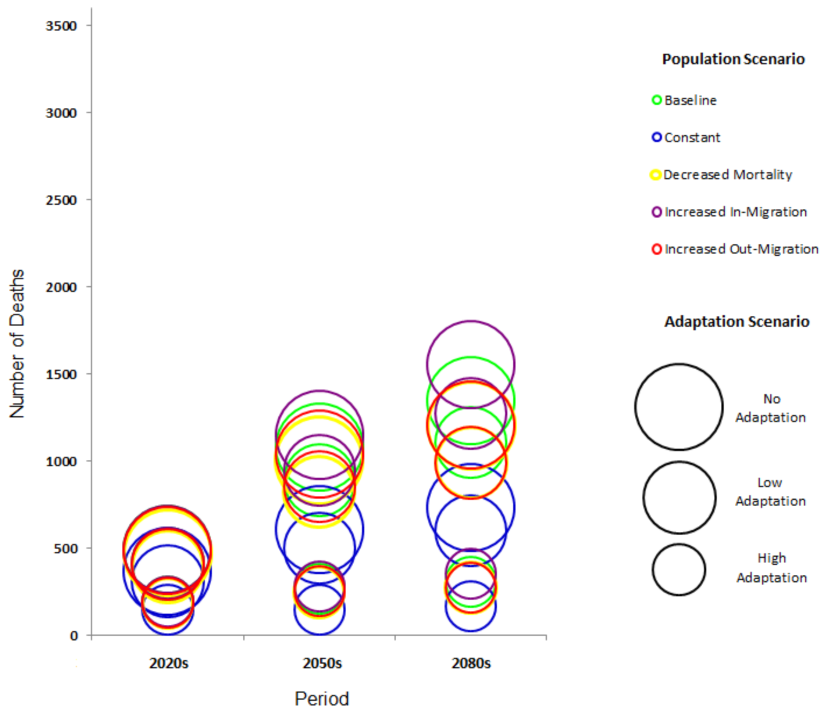

Panel B

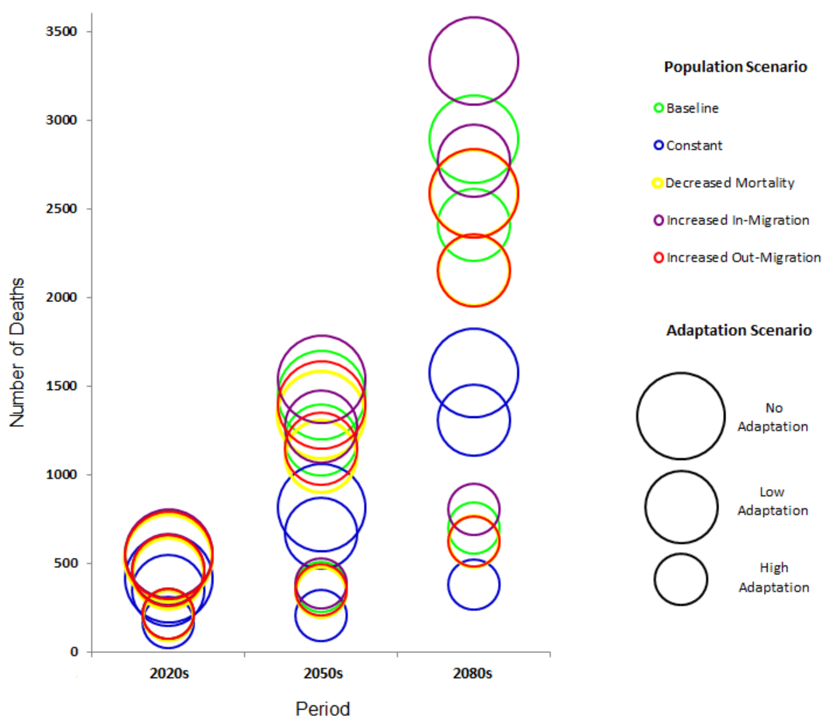

Environ Health Perspect
DOI: 10.1289/EHP166

Note to readers with disabilities: *EHP* strives to ensure that all journal content is accessible to all readers. However, some figures and Supplemental Material published in *EHP* articles may not conform to 508 standards due to the complexity of the information being presented. If you need assistance accessing journal content, please contact ehp508@niehs.nih.gov. Our staff will work with you to assess and meet your accessibility needs within 3 working days.

Supplemental Material

Towards More Comprehensive Projections of Urban Heat-Related Mortality: Estimates for New York City under Multiple Population, Adaptation, and Climate Scenarios

Elisaveta P. Petkova, Jan K. Vink, Radley M. Horton, Antonio Gasparrini, Daniel A. Bader, Joe D. Francis, and Patrick L. Kinney

Table of Contents

Table S1 Population scenarios and corresponding mortality rates used in this study.

YEAR	TOTAL POPULATION					ANNUAL MORTALITY RATES PER 100,000 POPULATION				
	Baseline [a]	***Decreased Mortality*** [b]	***Increased In-Migration*** [c]	***Increased Out-Migration*** [d]	***Constant*** [e]	***Baseline*** [a]	***Decreased Mortality*** [b]	***Increased In-Migration*** [c]	***Increased Out-Migration*** [d]	***Constant*** [e]
2010	8175133	8175133	8175133	8175133	8175133	652	650	652	652	652
2011	8238516	8238709	8240542	8237833	8175133	663	658	662	663	652
2012	8299751	8300330	8305808	8297714	8175133	673	667	673	674	652
2013	8358916	8360053	8370952	8354845	8175133	684	674	683	684	652
2014	8416212	8418107	8436143	8409457	8175133	694	682	692	694	652
2015	8471895	8474727	8501573	8461805	8175133	703	690	701	704	652
2016	8525758	8529698	8566979	8511698	8175133	712	697	710	713	652
2017	8577624	8582850	8632145	8558967	8175133	722	704	719	723	652
2018	8627530	8634209	8697063	8603663	8175133	732	712	727	733	652
2019	8675385	8683689	8761587	8645717	8175133	742	720	737	744	652
2020	8721390	8731487	8825880	8685346	8175133	753	729	747	755	652
2021	8765407	8777459	8889749	8722415	8175133	764	737	757	766	652
2022	8807304	8821478	8953018	8756805	8175133	776	747	767	778	652
2023	8847177	8863632	9015724	8788634	8175133	787	755	777	789	652
2024	8885095	8904000	9077902	8817986	8175133	799	765	787	801	652
2025	8921033	8942541	9139465	8844840	8175133	810	774	797	813	652
2026	8955053	8979326	9200435	8869289	8175133	822	784	808	826	652
2027	8987124	9014321	9260734	8891300	8175133	835	794	819	839	652
2028	9017255	9047537	9320328	8910900	8175133	847	804	829	851	652
2029	9045059	9078585	9378773	8927697	8175133	860	814	840	864	652
2030	9070840	9107764	9436322	8941997	8175133	872	824	851	878	652
2031	9094849	9135329	9492240	8954104	8175133	886	836	863	892	652

2032	9117093	9161272	9546449	8964009	8175133	899	847	874	906	652
2033	9137532	9185551	9598910	8971675	8175133	911	856	884	918	652
2034	9156274	9208290	9649722	8977270	8175133	923	865	893	930	652
2035	9173495	9229616	9699028	8980940	8175133	933	873	901	940	652
2036	9189405	9249750	9747035	8982920	8175133	942	880	909	950	652
2037	9204070	9268746	9793792	8983284	8175133	951	887	916	960	652
2038	9217617	9286727	9839423	8982187	8175133	960	894	923	969	652
2039	9230091	9303731	9883955	8979663	8175133	969	901	930	978	652
2040	9241489	9319745	9927365	8975731	8175133	976	906	936	986	652
2041	9251864	9334821	9969700	8970459	8175133	983	911	941	993	652
2042	9261278	9349010	10011018	8963915	8175133	989	916	946	1000	652
2043	9269889	9362449	10051431	8956269	8175133	994	919	950	1006	652
2044	9277759	9375207	10090994	8947607	8175133	1000	923	954	1012	652
2045	9284976	9387365	10129789	8938033	8175133	1004	925	957	1016	652
2046	9291622	9398996	10167893	8927644	8175133	1007	927	959	1020	652
2047	9297761	9410160	10205342	8916493	8175133	1011	929	962	1024	652
2048	9303433	9420886	10242175	8904659	8175133	1014	930	964	1027	652
2049	9308625	9431151	10278357	8892114	8175133	1016	931	966	1031	652
2050	9313369	9440993	10313920	8878911	8175133	1018	931	967	1032	652
2051	9317783	9450544	10348974	8865197	8175133	1019	931	967	1034	652
2052	9321906	9459819	10383544	8851010	8175133	1020	931	968	1036	652
2053	9325826	9468910	10417712	8836440	8175133	1022	931	969	1038	652
2054	9329481	9477757	10451402	8821437	8175133	1025	932	971	1040	652
2055	9332831	9486325	10484576	8805989	8175133	1026	932	972	1042	652
2056	9335894	9494642	10517243	8790111	8175133	1027	931	973	1043	652
2057	9338741	9502772	10549459	8773891	8175133	1028	930	974	1045	652

2058	9341456	9510800	10581307	8757412	8175133	1029	930	975	1046	652
2059	9344020	9518696	10612754	8740664	8175133	1032	930	976	1048	652
2060	9346395	9526449	10643766	8723626	8175133	1034	930	978	1050	652
2061	9348520	9533991	10674329	8706244	8175133	1036	931	980	1053	652
2062	9350392	9541313	10704452	8688518	8175133	1038	932	983	1055	652
2063	9351992	9548412	10734106	8670448	8175133	1041	932	985	1058	652
2064	9353286	9555243	10763252	8651992	8175133	1044	933	988	1061	652
2065	9354309	9561832	10791907	8633189	8175133	1047	934	991	1064	652
2066	9355007	9568146	10820021	8614023	8175133	1049	935	993	1066	652
2067	9355461	9574235	10847659	8594561	8175133	1051	935	995	1068	652
2068	9355685	9580136	10874853	8574832	8175133	1052	935	997	1069	652
2069	9355708	9585856	10901614	8554869	8175133	1054	935	999	1071	652
2070	9355566	9591414	10927984	8534707	8175133	1055	934	1000	1071	652
2071	9355290	9596846	10953987	8514390	8175133	1055	933	1001	1071	652
2072	9354935	9602203	10979675	8493968	8175133	1055	931	1001	1071	652
2073	9354541	9607530	11005096	8473499	8175133	1055	930	1002	1071	652
2074	9354144	9612840	11030284	8453014	8175133	1054	928	1002	1070	652
2075	9353765	9618152	11055246	8432517	8175133	1054	926	1002	1069	652
2076	9353405	9623494	11080008	8412056	8175133	1053	924	1002	1068	652
2077	9353110	9628889	11104603	8391647	8175133	1052	921	1002	1067	652
2078	9352922	9634378	11129069	8371325	8175133	1051	919	1002	1065	652
2079	9352842	9639977	11153430	8351130	8175133	1049	916	1002	1064	652
2080	9352876	9645697	11177693	8331045	8175133	1048	913	1001	1062	652
2081	9353015	9651530	11201852	8311075	8175133	1047	911	1001	1061	652
2082	9353268	9657484	11225923	8291215	8175133	1046	908	1001	1059	652
2083	9353616	9663551	11249877	8271464	8175133	1045	906	1001	1058	652

2084	9354054	9669718	11273722	8251808	8175133	1045	903	1001	1057	652
2085	9354555	9675981	11297444	8232243	8175133	1044	901	1001	1056	652
2086	9355110	9682332	11321033	8212757	8175133	1044	899	1002	1055	652
2087	9355709	9688761	11344496	8193341	8175133	1044	897	1002	1055	652
2088	9356337	9695256	11367821	8173985	8175133	1043	894	1002	1054	652
2089	9356981	9701808	11390996	8154679	8175133	1043	892	1003	1054	652
2090	9357622	9708412	11414014	8135407	8175133	1043	891	1004	1053	652
2091	9358255	9715049	11436862	8116171	8175133	1044	889	1004	1053	652
2092	9358866	9721707	11459546	8096959	8175133	1044	887	1005	1053	652
2093	9359453	9728390	11482065	8077773	8175133	1044	885	1005	1053	652
2094	9360006	9735084	11504414	8058587	8175133	1045	884	1006	1053	652
2095	9360502	9741785	11526581	8039417	8175133	1045	882	1007	1053	652
2096	9360944	9748471	11548566	8020245	8175133	1046	881	1008	1053	652
2097	9361320	9755136	11570353	8001060	8175133	1046	879	1009	1053	652
2098	9361633	9761789	11591959	7981876	8175133	1047	877	1009	1053	652
2099	9361885	9768438	11613408	7962707	8175133	1047	876	1010	1052	652

Population scenarios:

[a] *Baseline:* assumed that all parameters of the model remain constant, that is age specific fertility and mortality rates and age characteristics of migration are all kept constant, but the population ages forward;

[b] *Decreased Mortality*: assumed a decrease in age specific mortality rates such that the values reach to 2/3 of the 2010 values by 2100;

[c] *Increased In-Migration*: assumed that the growth of the domestic in-migration (from other parts of the US to NYC) will be half of the growth of the US population and that the growth of the international in-migration (from outside of the US to NYC) will be half of the growth of the projected international in-migration nationwide;

[d] *Increased Out-Migration*: assumed that the rate of out-migration would increase by 25% over the projection period;

[e] *Constant*: assumed that population and age of the population remains constant at the 2010 level.